Appl Magn Reson (2017) 48:715–722
DOI 10.1007/s00723-017-0889-6

Applied Magnetic Resonance

ORIGINAL PAPER

NMR Relaxation Efficiency of Aqueous Solutions of Composite $Mg_xZn_yFe_{3-x-y}O_4$ Nanoparticles

Yu. V. Bogachev[1] · A. V. Nikitina[1] · A. A. Kostina[1] · V. A. Sabitova[1] · V. V. Pankov[2] · T. G. Shutava[3] · E. G. Petrova[2] · D. A. Kotsikau[2] · V. O. Natarov[2] · K. S. Livanovich[3]

Received: 29 January 2017 / Revised: 20 April 2017 / Published online: 11 May 2017

Abstract The results of proton nuclear magnetic resonance (NMR) relaxation measurements in aqueous solutions of $Mg_xZn_yFe_{3-x-y}O_4$ magnetite-based composite magnetic nanoparticles (MNPs) are discussed. It is shown that their transverse relaxivity (relaxation efficiency) r_2 is significantly higher than the longitudinal relaxivity r_1 and depends on the magnetic nanoparticles composition and preparation method. A polyelectrolyte layer adsorbed on the nanoparticle surface increases both relaxivity values. The carbonate-synthesized MNPs possess higher values of r_2 and r_1 as compared with base-precipitated complex oxides. Relaxivity r_2 is shown to be affected by stability of MNPs in aqueous solutions and the aggregation behavior apparently can be assessed through the NMR relaxation measurements.

✉ Yu. V. Bogachev
Yu.Bogachev@mail.ru

V. V. Pankov
pankov@bsu.by

T. G. Shutava
shutova@ichnm.basnet.by

[1] Department of Physics, Saint-Petersburg Electrotechnical University "LETI", 5, prof. Popov St., Saint-Petersburg 197376, Russia

[2] Department of Chemistry, Belarusian State University, 4, Nezavisimosti Av., 220030 Minsk, Belarus

[3] Institute of Chemistry of New Materials, National Academy of Sciences of Belarus, 36, F. Skaryna St., 220141 Minsk, Belarus

1 Introduction

Nowadays, application of magnetic nanoparticles (MNPs) in medicine and biology, i.e., for diagnostics, magnetic separation, drug delivery, etc., persistently widens [1–3]. The use of MNPs in magnetic resonance (MR) diagnostics in both in vivo [4] and in vitro [5, 6] modes is of particular interest. To be applicable in MR diagnostics, magnetic nanoparticles are required to possess the following properties: certain magnetic characteristics, colloidal stability (high aggregation stability), biocompatibility, low toxicity, and functionalized surface to target specific biological objects.

Conventionally used for MR diagnostics nanoparticles are superparamagnetic iron oxide particles in the matrices of dextran, carboxydextran, polyethylene glycol (PEG) modified polysaccharide [7–10], and silicon oxide [11–13]. The magnetic properties of the nanoparticles are affected by the degree of core crystallinity and size that depend on the method of MNPs' synthesis, as well as on the shell composition and thickness governing also dispersibility, aggregation stability of the particles in aqueous solutions, and their interaction with cell and tissue [14, 15]. Though Fe_3O_4 nanoparticles exhibit good r_2 relaxivity, it may not be sufficient for MR imaging (MRI). Therefore, the development of new types of nanoparticles is particularly important. In this regard, a metal dopant substitution strategy of metal ferrite nanoparticles has been pursued to achieve high and tunable nanomagnetism. For example, nanoparticles with tunable magnetism, such as manganese-doped metal ferrite nanoparticles, have enhanced MRI contrast effects as compared with the conventional iron oxide nanoparticles [16].

One of the most common methods of iron oxide-based MNPs' synthesis is co-precipitation of metal ions from their salt solutions. Due to high sensitivity of the method to different parameters (nature of precipitant, reagents concentration, temperature of synthesis, pH of the reaction medium, etc.), it allows to vary widely the size and properties of the produced nanoparticles [2, 3].

The aim of this work is to study the NMR relaxation properties of protons in aqueous solutions in the presence of composite nanoparticles based on solid solutions of zinc, magnesium, and iron oxides. An efficient way to estimate the NMR relaxation properties would be to calculate their longitudinal r_1 and transverse r_2 relaxivities.

2 Experimental Methods

Composite MNPs based on magnetite doped with zinc and/or magnesium with a general composition of $Mg_xZn_yFe_{3-x-y}O_4$ were obtained by co-precipitation from solutions of the corresponding salts using NaOH and Na_2CO_3 as precipitants. A solution of reagents mixed in a stoichiometric ratio was introduced at room temperature into the solution of precipitant, taken with some excess, and left for 1 h under intensive mixing until the crystallization process was complete. The pH of the system during the reaction was maintained at $\sim$11, allowing to achieve full

deprotonation of aqua complexes of all metal ions without formation of water-soluble hydroxocomplexes. In the case of carbonate co-precipitation, the reaction mixture was rapidly heated up to a temperature of 90 °C and then allowed to cool down to room temperature. The resulting precipitate was then washed by magnetic decantation. The nomenclature of the samples is given in Table 1.

Magnetic nanoparticles functionalized with a layer of poly(diallyldimethylammonium chloride) (PDDA, 100–200 kDa, Sigma) were prepared by dispersing MNPs' powder (0.1 ÷ 0.3 mg/mL) in a PDDA solution with a tenfold mass excess of the polyelectrolyte over MNPs [17]. A suspensions was treated for 2 min in a Sapphir ultrasonic bath, Russia, 4–5 times for 45 s by submersible ultrasonic disperser USG-13-0,1/22, Russia, and, finally, for 2 min in the ultrasonic bath. To prevent overheating upon ultrasonication, the samples were cooled in an ice bath. Modified nanoparticles were separated by centrifugation (a Z36HK Hermle centrifuge, Germany) and then dispersed in distilled water.

X-ray diffraction (XRD) patterns of the powdered samples were recorded on a DRON-2.0 diffractometer (Co Kα-radiation) in the range $2\Theta = 20°–90°$. Size and morphology of the particles were examined by scanning (SEM) and transmission electron microscopy (TEM) using LEO 906E, JOEL EM100 CX and LEO 1420 microscopes. Magnetic characteristics of nanoparticles including saturation magnetization M_s were measured using a Cryogen Free Measurement System by Cryogenic Ltd ($T = 7–300$ K, $H_{max} = 18$ T).

Scanning probe microscopy (SPM) images of nanoparticles were recorded on a Multi Mode Nanoscope III (Veeco, USA) microscope in a height mode. The scanning speed was 3–5 Hz; silicon nitride cantilever with a stiffness constant of 0.12 N/m was used. The information density was 512 × 512 pixels. The images were processed using the Nanoscope v531 software.

The average hydrodynamic diameter Z_{av}, polydispersity index (PDI), and ζ-potential of particles were determined on a Zetasizer Nano ZS, Malvern, USA analyzer. The size distribution of nanoparticles was obtained using the standard instruments software. The number weighted size distribution of nanoparticles was obtained using the standard instruments software. The mean diameter d_N characterizes the most abundant size of nanoparticles.

Table 1 Composition, physicochemical properties, and NMR relaxivity of the investigated composite systems

No.	MNPs' composition	Method of synthesis	M_s, emu/g	Z_{av}, nm	PDI	d_N, nm	r, mM^{-1} s^{-1}		r_2/r_1
							r_2	r_1	
$Mg_xZn_yFe_{3-x-y}O_4$/PDDA nanoparticles									
1	Fe_3O_4	Carbonate precipitation	63 ± 2	126 ± 11	0.26 ± 0.04	75 ± 2	Var	Var	Var
2	$Mg_{0.1}Fe_{2.9}O_4$		65 ± 2	147 ± 6	0.23 ± 0.01	61 ± 3	302 ± 15	34 ± 2	8.9
3	$Mg_{0.1}Zn_{0.2}Fe_{2.7}O_4$		59 ± 2	252 ± 36	0.37 ± 0.05	61 ± 3	261 ± 13	43 ± 2	6.1
4	$Mg_{0.12}Zn_{0.08}Fe_{2.8}O_4$		59 ± 2	201 ± 27	0.32 ± 0.01	73 ± 3	Var	Var	Var
5	$Mg_{0.1}Fe_{2.9}O_4$	Alkaline precipitation	29 ± 1	120 ± 25	0.25 ± 0.08	80 ± 3	78 ± 3	15 ± 0.8	5.1
6	$Mg_{0.12}Zn_{0.08}Fe_{2.8}O_4$		34 ± 1	237 ± 61	0.49 ± 0.10	86 ± 3	146 ± 7	32 ± 1	4.6

The NMR measurements were performed using a Spin Track NMR relaxometer, Russia, with the magnitude of magnetic field of 0.33 T that corresponds to a proton resonance frequency of 14 MHz. To measure the spin–lattice relaxation time T_1, an inversion-recovery (180°–τ–90°) pulse sequence was used. To measure the spin–spin relaxation time T_2, the Carr–Purcell–Meiboom–Gill (CPMG) pulse sequence was used. The pulse durations were equal to 2.6 and 5.2 μs for the 90° and 180° pulses, respectively. The relaxation times were calculated from the magnetization recovery curves for the samples. The relaxation behavior for the both longitude and transverse magnetizations is monoexponential. The potential effectiveness of contrasting MR images by composite nanoparticles solution was characterized by the relaxivity (relaxation efficiency) r, the magnitude of which is the proportionality constant of the measured rate of relaxation, or R_1 ($1/T_1$) and R_2 ($1/T_2$), over a range of contrast agent concentrations.

The total concentration of iron in MNPs' dispersions was determined using o-phenanthroline [18]. The nanoparticles were dissolved in a 5 M HCl solution at 70 °C, and the acid was further neutralized with an NaOH solution to pH 4–5. The spectra of solutions in the visible region were recorded on a CM2203 Solar, Belarus spectrofluorimeter.

3 Results and Discussion

The results of XRD studies confirm the formation of single-phase crystalline compounds with a spinel structure upon both alkaline and carbonate co-precipitation of iron, magnesium, and zinc salts. According to electron microscopy, the average grain size for the precipitates is ~10 and ~20 nm for alkaline and carbonate precipitation, respectively (Fig. 1). At room temperature, all the investigated magnetic materials demonstrate superparamagnetic behavior with no coercivity and remanent magnetization. The saturation magnetization values of the nanomaterials as well as other physicochemical properties are presented in Table 1.

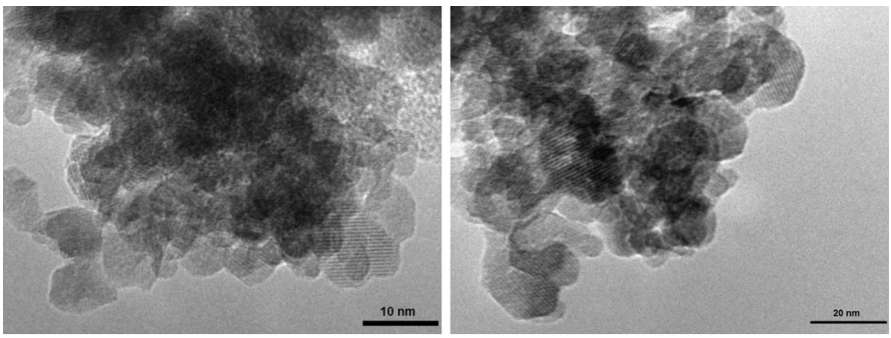

Fig. 1 Typical TEM image of $Mg_xZn_yFe_{3-x-y}O_4$ nanoparticles obtained by alkaline (**a**) and carbonate (**b**) co-precipitation

Aqueous suspensions of MNPs' powders as prepared are characterized by multimodal size distribution with a high polydispersity index (PDI > 0.4) and sedimentation instability (Table 1). Stable suspensions with a narrow size distribution (PDI < 0.250) were obtained by dispersing MNPs' powders in a PDDA solution (Table 1). In the colloids of PDDA-modified nanoparticles, the most abundant fraction of particles has d_N in the range of 60–86 nm. The average dynamic light scattering (DLS) diameter of the nanoparticles Z_{av} does not exceed 250 nm and characterizes the size of the cores along with coating polyelectrolyte material (PDDA) and a solvent layer attached to the particles when they are considered under Brownian motion as ideal spheres. The observed difference between d_N and Z_{av} is associated with the increased contribution of large particles in a polydisperse sample into dynamic light scattering. The nanoparticles coated with a PDDA layer have a high positive zeta potential value, $+30 \div 50$ mV, indicating that PDDA firmly envelops the particle and supporting their high colloidal stability for a long time.

According to SPM (Fig. 2), in all the MNPs coated with a PDDA layer, the major fraction of nanoparticles with a size within 30–60 nm is supplemented by fraction of smaller nanoparticles with a diameter lower than 30 nm. Some bigger particles and agglomerates ($\sim$200 nm) are probably formed during sample preparation. The size of nanoparticles estimated by SPM correlates well with the MNPs' diameter distribution calculated from DLS experiments (Table 1).

The thickness of an adsorbed layer of PDDA on a surface is less than 1 nm [19]. Polyelectrolyte layers are permeable to low molecular weight compounds [20], so PDDA influence on the diffusion of water molecules to the surface of the MNPs is apparently negligible.

Figure 3 represents the longitudinal $R_1 = 1/T_1$ and transverse $R_2 = 1/T_2$ NMR relaxation rates of protons in aqueous solution of MNPs' plotted versus the concentration of MNPs.

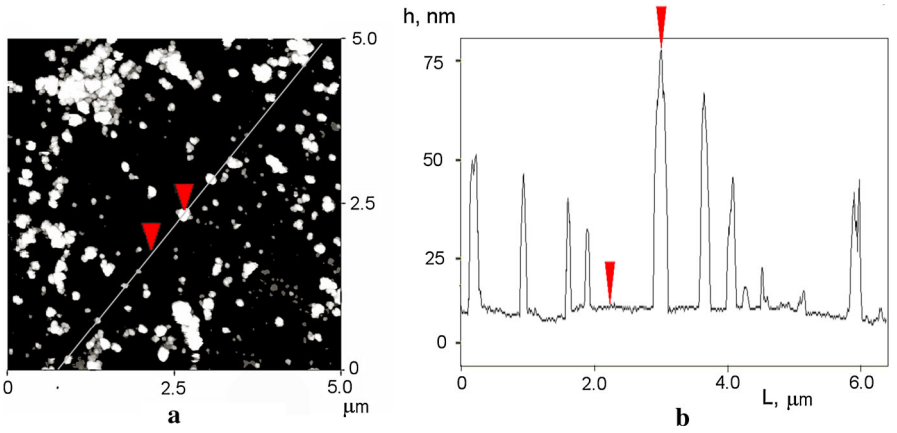

Fig. 2 **a** SPM image of Fe_3O_4 nanoparticles coated with a PDDA layer and **b** height profile across the indicated line

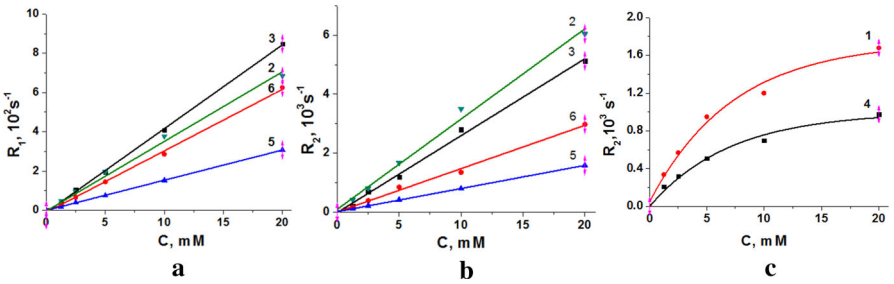

Fig. 3 Dependence of the longitudinal R_1 (**a**) and transverse R_2 (**b**, **c**) relaxation rates of protons in aqueous solution on the MNPs' concentration. The numbering of the samples is the same as in Table 1

For most samples, studied graphic dependences $R_i(C)$ are linear (Fig. 3a, b) and described by the functions $R_i = r_i \cdot C + R_{0i}$, where C is the concentration of MNPs, R_{0i} is the constant determined by the relaxation rate of water protons in the absence of MNPs ($R_{01} = 0.5\ c^{-1}$, $R_{02} = 3\ c^{-1}$ for the studied samples), and r_i is the relaxivity. For such samples, the relaxivity is defined as the tangent of the slope of the straight line $R_i(C)$ and has a constant value. The results of r_1 and r_2 calculations for samples 2, 3, 5, and 6 are given in Table 1.

For two samples of MNPs synthesized with carbonate, 1 and 4, the dependences of the transverse relaxation rates R_2 of water protons on the MNPs' concentration are non-linear (Fig. 3c). The analysis of these non-linear $R_2(C)$ dependencies allows us to determine the relaxivity r_2 as a derivative of the experimental curve $R_2(C)$ at a given point [100]. The calculation results show that for samples 1 and 4, relaxivity r_2 is variable and decreases with increase in the MNPs' concentration. The observed phenomenon was attributed to instability of these MNPs in aqueous solution and their ability to form clusters as the MNPs' concentration in the solution increases. This effect of MNPs' clustering was observed visually for the mentioned samples and increased with increasing residence time of the sample in the magnetic field of the NMR relaxometer. Similar results were obtained earlier in the NMR relaxation study of protons in aqueous solutions of iron oxide MNPs with Si–C shell [11]. The aggregation of the nanoparticles affects the outer-sphere proton relaxation processes and as well as the diffusion of protons in the vicinity of magnetic centers, resulting in lower relaxation rates as compared with single nanoparticles.

From the analysis of the experimental data for substituted magnetite MNPs in aqueous solutions (Table 1), the following conclusions can be made.

1. For all investigated $Mg_xZn_yFe_{3-x-y}O_4$ compositions regardless of preparation technique, the transverse relaxivity r_2 is considerably higher than the longitudinal relaxivity r_1. Typical contrast agents with an r_2/r_1 ratio in the range of 2–40 are considered as T_2 contrast agents, while for T_1 contrast agents, this ratio is usually lower [10]. Thus, the investigated MNPs can be potentially used as negative contrast agents in MRI diagnostics [14].
2. In spite of having comparable hydrodynamic diameters, $Mg_xZn_yFe_{3-x-y}O_4$/PDDA nanoparticles obtained by co-precipitation with carbonate possess higher relaxivities r_1 and r_2 than alkaline-prepared MNPs.

3. The transverse relaxivity r_2 for the stable colloidal systems (samples 2, 3, 5, 6) was found to be in a linear dependence with a saturation magnetization value of the MNPs' magnetic core. This means that higher values of saturation magnetization are higher values of transverse relaxivity.
4. By relaxation characteristics, PDDA-coated $Mg_xZn_yFe_{3-x-y}O_4$ MNPs are comparable, and even superior, to some commercial contrast agents based on superparamagnetic iron oxide nanoparticles, such as Ferridex (particle size of 120–190 nm, $r_2 = 98.3\ mM^{-1}\ s^{-1,}$ $r_2/r_1 = 4.1$) and Resovist (particle size 40–60 nm, $r_2 = 150.0\ mM^{-1}\ s^{-1)}$. Apparently, this is due to the larger size of the oxide magnetic cores, because both relaxivity values r_1 and r_2 tend to increase as the magnetic core dimensions increase [12]. The reported diameter of iron oxide crystals in the commercial preparations mentioned above is from 4.2 to 5.6 nm [7], and larger nanoparticles have a higher magnetization efficiency and stronger contrasting effect [15].
5. A water-saturated layer of strong polyelectrolyte PDDA adsorbed on the MNPs' surface enhances colloidal stability of nanoparticles and probably facilitates the proton exchange in the vicinity of MNPs' surface, thus increasing r_2 relaxivity of PDDA-coated nanoparticles as compared with uncoated ones.

4 Conclusions

The study of the NMR relaxation of protons in aqueous solutions of composite magnetite-based MNPs shows that their relaxation efficiency r_2 is much higher than relaxation efficiency r_1 and depends on the composition and method of MNPs' synthesis. The colloidal stability of nanoparticles and their relaxation characteristics can be improved by adsorbing a layer of strong polyelectrolyte on the MNPs' surface. The aggregation behavior of MNPs/PDDA in aqueous solutions can be evaluated through measuring concentration dependences of R_2 relaxation rates. The $Mg_xZn_yFe_{3-x-y}O_4$/PDDA nanoparticles can be applicable in the development of negative contrast agents for MRI diagnostics.

Acknowledgements Part of this work was supported by the Ministry of Education and Science of the Russian Federation (Project 3.6522.2017).

References

1. J. Gao, H. Gu, B. Hu, Acc. Chem. Res. **42**(8), 1097 (2009)
2. S. Laurent, D. Forge, M. Port, A. Roch, C. Robick, L.V. Elst, R.N. Muller, Chem. Rev. **108**, 2064 (2008)
3. A.H. Lu, E.L. Salabas, F. Schuth, Angew. Chem. Int. Ed. **46**, 1222 (2007)
4. R. Thomas, I.K. Park, Y. Jeong, Int. J. Mol. Sci. **14**, 15910 (2013)
5. H. Shao, C. Min, D. Issadore, M. Liong, J. Chung, R. Weissleder, H. Lee, Theranostics **2**(1), 55 (2012)
6. R. Hao, R. Xing, Z. Xu, Y. Hou, S. Gao, S. Sun, Adv. Mater. **22**(25), 2729 (2010)
7. Y.J. Wang, Quant. Imaging Med. Surg. **1**(1), 35 (2011)
8. B. Issa, S. Qadri, I.M. Obaidat, R.W. Bowtell, Y. Haik, J. Magn. Reson. Imaging **34**(5), 1192 (2011)

9. L.E.W. La Conte, N. Nitin, O. Zurkiya, D. Caruntu, C.J. O'Connor, X. Hu, G. Bao, J. Magn. Reson. Imaging **26**(6), 1634 (2007)
10. M.F. Casula, A. Corrias, P. Arosio, A. Lascialfari, T. Sen, P. Floris, J. Colloid Interface Sci. **357**(1), 50 (2011)
11. Y.V. Bogachev, J.S. Chernenko, K.G. Gareev, I.E. Kononova, L.B. Matyushkin, V.A. Moshnikov, S.S. Nalimova, Appl. Magn. Reson. **45**, 329 (2014)
12. T. Ahmad, H. Bae, I. Rhee, Y. Chang, J. Lee, S. Hong, Curr. Appl. Phys. **12**(3), 969–974 (2012)
13. M.F. Casula, A. Corrias, P. Arosio, A. Lascialfari, T. Sen, P. Floris, J. Colloid Interface Sci. **357**(1), 50 (2011)
14. Z.R. Stephen, F.M. Kievit, M. Zhang, Mater. Today **14**(7–8), 331 (2011)
15. H.B. Na, T. Hyeon, in *Nanoplatform-Based Molecular Imaging*, ed. by X. Chen (Willey, New Jersey, 2011). doi:10.1002/9780470767047.ch13
16. J. Jang, H. Nah, J.H. Lee, S.H. Moon, M.G. Kim, J. Cheon, Angew. Chem. **121**, 1260 (2009)
17. V.V. Pankov, T.G. Shutava, K.S. Livanovich, D.A. Kotsikau, E.G. Petrova, V.O. Natarov, S.V. Trukhanov. Proceedings of the National Academy of Sciences of Belarus. Series of Chemical Sciences, no. 2, pp. 19–24 (2017) **(in Russian)**
18. Yu.A. Moryganova, V.L. Menshikova, V.N. Kuleshov, V.F. Ochkov, B.S. Fedoseev, *Chemical Analysis in Energetics. Book 1: Photometry. Book 2: Titrimetry and Gravimetry* (MEI, Moscow, 2008), p. 407 **(in Russian)**
19. H.N. Tien, A. Ottova-Leitmannova, in *Planar Lipid Bilayers (BLM's) and Their Applications*, vol 7. (Elsevier Science, London, 2003), p. 1044. ISBN: 9780080539034
20. B.G. De Geest, S. De Koker, G.B. Sukhorukov, O. Kreft, W.J. Parek, A.J. Skirtach, J. Demeester, S.S. De Smedt, W.E. Hennink, Soft Matter **5**(2), 282 (2009)